Frequency response of cantilever beams immersed in viscous fluids with applications to the atomic force microscope

John Elie Sader

Citation: J. Appl. Phys. **84**, 64 (1998); doi: 10.1063/1.368002
View online: http://dx.doi.org/10.1063/1.368002
View Table of Contents: http://jap.aip.org/resource/1/JAPIAU/v84/i1
Published by the American Institute of Physics.

Frequency response of cantilever beams immersed in viscous fluids with applications to the atomic force microscope

John Elie Sader[a)]
Department of Mathematics and Statistics, University of Melbourne, Parkville, 3052, Victoria, Australia

(Received 30 December 1997; accepted for publication 30 March 1998)

The vibrational characteristics of a cantilever beam are well known to strongly depend on the fluid in which the beam is immersed. In this paper, we present a detailed theoretical analysis of the frequency response of a cantilever beam, that is immersed in a viscous fluid and excited by an arbitrary driving force. Due to its practical importance in application to the atomic force microscope (AFM), we consider in detail the special case of a cantilever beam that is excited by a thermal driving force. This will incorporate the presentation of explicit analytical formulae and numerical results, which will be of value to the users and designers of AFM cantilever beams. © *1998 American Institute of Physics.* [S0021-8979(98)03213-7]

I. INTRODUCTION

It is well known that the frequency response of an elastic beam, due to an external driving force, is strongly dependent on the fluid in which it is immersed.[1–25] In the absence of the fluid (i.e., in vacuum), analysis of the natural resonant frequencies of the beam is routine, and can be solved using simple analytical techniques in many cases of practical interest.[26] In contrast, the calculation of the frequency response of an elastic beam immersed in a viscous fluid poses a formidable challenge, and to date neither an analytical nor numerical solution to the problem, which rigorously accounts for the effects of viscosity, has appeared in the literature. At this stage we must emphasize that numerous theoretical studies have been carried out with the assumption that the fluid is inviscid in nature (see Refs. 1, 2, 4, 7–11, 15, 22, 24), a justifiable approach in many cases of practical interest, as we shall discuss. However, for situations where structural and radiation damping are negligible in comparison to dissipative viscous effects in the fluid,[27] these approaches are clearly incapable of giving any information about the total frequency response of the beam, and consequently only indicate the positions of the resonance peaks. Furthermore, these approaches can lead to significant errors in the positions of the resonance peaks, depending on the dimensions of the beam, as we shall discuss in detail. This is particularly true for cantilever beams used in the atomic force microscope (AFM). We now note that to our knowledge the only model that includes the effects of viscosity is the heuristic approach of approximating the beam by a sphere.[14,16,21] Clearly, such an approach is unsatisfactory, since it does not rigorously account for the true geometry of the beam. Therefore, it is highly desirable to have a rigorous theoretical model that accurately accounts for viscous effects in the fluid.

In this article, we present a general theoretical model for the frequency response of a cantilever beam of arbitrary cross section, which is excited by an arbitrary driving force, and immersed in a viscous fluid of arbitrary density and viscosity. We emphasize that the fundamental restrictions on the analysis are that the amplitude of vibration must be small, the fluid must be incompressible, and the length of the beam must greatly exceed its nominal width, as we shall discuss in detail. The formulation for a general cross section is then made possible by the specification of a ''hydrodynamic function'' which accounts for the geometry of the cross section of the beam. Depending on the cross section of the beam, this hydrodynamic function can be calculated analytically or numerically, as we shall discuss. Since beams that are rectangular or circular in cross section are of considerable practical interest in many applications (e.g., see Refs. 2–6, 9, 12, 13, 15, 20, 28, 29), we shall give explicit analytical formulae for the hydrodynamic functions in both these cases.

Knowledge and understanding of the frequency spectra of cantilever beams excited by a thermal driving force is of fundamental practical importance in application to the AFM.[18,30,31] However, despite the significant amount of experimental work that has been carried out on this problem,[14,18,19,21,23] a theoretical model capable of predicting the observed spectra has hitherto remained elusive. At this stage, we note that a theoretical study of the thermal spectra of AFM cantilever beams recently appeared in the literature.[31] However, the model presented in Ref. 31 accounts for the hydrodynamic loading by assuming that only dissipative effects are present in the fluid, which are subsequently modeled in a simplistic fashion that involves an unknown fitting parameter. This fitting parameter is then calculated from knowledge of the quality factor of the frequency response, which is measured experimentally. Therefore, it is clear that the model presented in Ref. 31 cannot be used to give *a priori* predictions of the frequency spectra. In contrast, the present model rigorously accounts for both dissipative and inertial effects in the fluid, and is therefore capable of making detailed calculations of the thermal frequency spectra of AFM cantilever beams of arbitrary dimensions immersed in arbitrary viscous fluids. Using the present theoretical model, the frequency response is determined in an *a*

a)Electronic mail: elie@maths.mu.oz.au

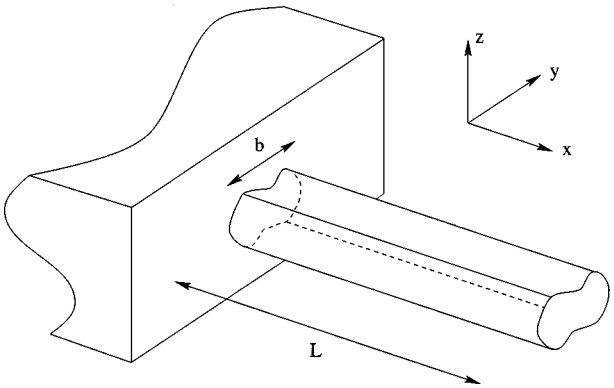

FIG. 1. Figure of cantilever beam with uniform arbitrary cross section showing length L, nominal width b and coordinate system. The origin of the coordinate system is at the center of mass of the cross section of the beam, at its clamped end.

priori manner from the material and geometric properties of the beam and the density and viscosity of the fluid.

At this stage we note that in many experimental and theoretical treatments to date it has been assumed that in the neighborhood of a resonance peak the thermal frequency spectrum of a cantilever beam is well approximated by that of a simple harmonic oscillator (SHO).[14,18,32] Using the present theoretical model, we rigorously show that this hypothesis is only valid in the case where dissipative effects in the fluid can be considered to be small. If this latter condition is not satisfied, however, then such an analogy is not possible. Consequently, we give explicit analytical formulae for the quality factor and resonant frequency of the frequency response in the case where dissipative effects in the fluid are small but finite, results which to date have remained elusive despite a considerable amount of research activity.[5,16,21,31] We also present detailed theoretical results for the thermal frequency spectra of cantilever beams immersed in gases and fluids of arbitrary properties, which will be of significant practical value to the users and designers of AFM cantilever beams. Finally, we note that a comparison and assessment of the present theoretical model with detailed experimental results shall be presented in Ref. 33.

II. PRELIMINARY DISCUSSION

We begin by discussing the general assumptions and approximations implemented in the present theoretical model. A schematic depiction of a cantilever beam of arbitrary cross section is given in Fig. 1, and it is assumed that the beam satisfies the following criterion:

(1) The cross section of the beam is uniform over its entire length;
(2) The length of the beam L greatly exceeds its nominal width b; see Fig. 1;
(3) The beam is an isotropic linearly elastic solid and internal frictional effects are negligible;
(4) The amplitude of vibration of the beam is far smaller than any length scale in the beam geometry.[34]

Furthermore, we shall neglect all torsional effects in the beam and only consider the flexural modes of vibration. In particular, we shall consider modes whose motion is strictly in the z-direction; see Fig. 1. We emphasize that the above stated assumptions and restrictions are satisfied in many situations of practical interest, including cantilever beams used in the AFM.

Since the amplitude of vibration is small, it then follows that all nonlinear convective inertial effects in the fluid can be neglected, and the hydrodynamic loading on the beam will be a linear function of its displacement. Also, it is a direct consequence of criterion (2) above, that the velocity field in the fluid will vary slowly along the length of the beam in comparison to chordwise variations across its width. This indicates that the dominant length scale in the hydrodynamic flow is the nominal width b. It then follows that the velocity field at any point along the beam is well approximated by that of an infinitely long rigid beam executing transverse oscillations with the same amplitude. At this stage, we note that this approximation is implemented in the derivation of the well-known inviscid result for a rectangular cantilever beam due to Chu,[1] for which good accuracy has been demonstrated in comparison to experimental measurements[2]

$$\frac{\omega_{\text{fluid}}}{\omega_{\text{vac}}}=\left(1+\frac{\pi\rho b}{4\rho_c h}\right)^{-1/2}, \tag{1}$$

where ω_{fluid} and ω_{vac} are the resonant frequencies in vacuum and fluid, respectively, ρ_c is the density of the beam, b and h are the width and thickness of the beam, and ρ is the density of the fluid.

The fluid in which the cantilever beam is immersed is also assumed to be incompressible in nature. This assumption is justifiable in many cases of practical interest, since it is typically found that the wavelength of vibration greatly exceeds the dominant length scale in the flow b, which in turn is much larger than the amplitude of vibration.[35,36] The assumption of incompressibility also holds for gases, provided the above conditions are satisfied and the dominant length scale in the flow b greatly exceeds the mean free path of the gas. If this latter constraint were not satisfied, the treatment of the gas as a continuum would not be justified. We note that these constraints are satisfied in most cases of practical interest but situations do arise, particularly at low gas pressures where the latter constraint is violated.

As discussed above, the inviscid fluid model of Chu,[1] Eq. (1), can and has been successfully used to predict the resonant frequencies of cantilever beams of rectangular cross section immersed in viscous fluids. We now examine the validity of approximating a viscous fluid by an inviscid fluid, as the dimensions of the beam are varied. Since the dominant length scale in the flow is the nominal width b, it then follows from the above discussion that the appropriate Reynolds number Re for flow[37] is given by

$$\text{Re}=\frac{\rho\omega b^2}{4\eta}, \tag{2}$$

where ρ and η are the density and viscosity of the fluid, respectively, whereas ω is a characteristic radial frequency of the vibration. Clearly, in the limit as $\text{Re}\to\infty$ the fluid can be considered to be inviscid in nature, and that for practical

cases where $\mathrm{Re} \gg 1$ the inviscid fluid model is applicable. However, if we approximate ω by the resonant frequency of the cantilever beam in vacuum, it becomes evident that a reduction in the dimensions of the beam will also result in a reduction in Re; this shall be discussed in detail in Sec. IV. Correspondingly, viscous effects in the fluid become increasingly important as the dimensions of the beam are reduced. For AFM cantilever beams, it is found that $\mathrm{Re} \sim O(1)$,[17] which indicates that the inviscid fluid model is not applicable, and if used will result in significant errors, as was demonstrated in Ref. 17. Furthermore, we note that by construction the inviscid fluid model Eq. (1) gives no information about the frequency spectrum but only indicates the position of the resonance peak. In this paper, we rigorously include the effects of viscosity and consequently present results for the total frequency spectrum of the cantilever beam, that are valid for all beam dimensions.

III. THEORY

A. General theory

In this section we present the general theory for the dynamic deflection of a cantilever beam immersed in a viscous fluid and excited by an arbitrary external driving force. As discussed above, the theory to be presented is applicable to beams of arbitrary cross section, that are uniform along their entire length. All other restrictions and assumptions are as discussed in the previous section.

To begin we examine the governing equation for the dynamic deflection function $w(x,t)$ of the beam[26]

$$EI \frac{\partial^4 w(x,t)}{\partial x^4} + \mu \frac{\partial^2 w(x,t)}{\partial t^2} = F(x,t), \tag{3}$$

where E is Young's modulus, I is the moment of inertial of the beam, μ is the mass per unit length of the beam, F is the external applied force per unit length, x is the spatial coordinate along the length of the beam, and t is time. The boundary conditions for Eq. (3) are the usual clamped and free end conditions

$$\left[w(x,t) = \frac{\partial w(x,t)}{\partial x} \right]_{x=0} = \left[\frac{\partial^2 w(x,t)}{\partial x^2} = \frac{\partial^3 w(x,t)}{\partial x^3} \right]_{x=L}, = 0, \tag{4}$$

where L is the length of the beam (see Fig. 1). We now scale the spatial variable x with the length of the beam L and take the Fourier transform of Eq. (3) to obtain

$$\frac{EI}{L^4} \frac{d^4 \hat{W}(x|\omega)}{dx^4} - \mu \omega^2 \hat{W}(x|\omega) = \hat{F}(x|\omega), \tag{5}$$

where

$$\hat{X} = \int_{-\infty}^{\infty} X e^{-i\omega t} dt \tag{6}$$

for any function of time X. For simplicity of notation, the spatial variable x in Eq. (5) refers to its scaled quantity; this convention shall be applied henceforth. We note that in contrast to Eq. (3), Eq. (5) is an ordinary differential equation in the scaled spatial variable x, and is parametric in the radial frequency variable ω. Since Eq. (5) is obtained by taking the Fourier transform of Eq. (3), it then follows that the boundary conditions for $\hat{W}(x|\omega)$ are identical to those for $w(x,t)$ given in Eq. (4), with all partial derivatives replaced by full derivatives and with the spatial variable replaced by its scaled quantity.

For a cantilever beam moving in a fluid, the external applied load $\hat{F}(x|\omega)$ can be separated into two contributions:

$$\hat{F}(x|\omega) = \hat{F}_{\mathrm{hydro}}(x|\omega) + \hat{F}_{\mathrm{drive}}(x|\omega). \tag{7}$$

The first component in Eq. (7) is a hydrodynamic loading component $\hat{F}_{\mathrm{hydro}}(x|\omega)$ due to the motion of the fluid around the beam, whereas the second term is a driving force $\hat{F}_{\mathrm{drive}}(x|\omega)$ that excites the beam. To proceed with the analysis, the general form of $\hat{F}_{\mathrm{hydro}}(x|\omega)$ is required. We therefore examine the Fourier transformed equations of motion for the fluid

$$\nabla \cdot \hat{\mathbf{u}} = 0, \quad -\nabla \hat{P} + \eta \nabla^2 \hat{\mathbf{u}} = -i\rho\omega\hat{\mathbf{u}}, \tag{8}$$

where $\hat{\mathbf{u}}$ is the velocity field, $\hat{P}$ is the pressure, ρ is the density of the fluid, and η its viscosity. Note that the nonlinear convective inertial term is neglected in Eq. (8), for reasons discussed in the preceding section.

It is evident from Eq. (8) and the discussion given in Sec. II that the general form of $\hat{F}_{\mathrm{hydro}}(x|\omega)$ is given by

$$\hat{F}_{\mathrm{hydro}}(x|\omega) = \frac{\pi}{4} \rho \omega^2 b^2 \Gamma(\omega) \hat{W}(x|\omega), \tag{9}$$

where the ''hydrodynamic function'' $\Gamma(\omega)$ is dimensionless and is obtained from the solution of Eq. (8) for a rigid beam, with identical cross section to that of the cantilever beam, undergoing transverse oscillatory motion. The constant b in Eq. (9) is the dominant length scale in the hydrodynamic flow, as discussed above, which for a circular cylinder is its diameter, whereas for a rectangular beam is its width. We shall examine the explicit form of the hydrodynamic function for these two cases in Sec. III B.

Substituting Eq. (9) into (5) and rearranging we find

$$\frac{d^4 \hat{W}(x|\omega)}{dx^4} - \frac{\mu \omega^2 L^4}{EI} \left(1 + \frac{\pi \rho b^2}{4\mu} \Gamma(\omega) \right) \hat{W}(x|\omega) = \hat{s}(x|\omega), \tag{10}$$

where

$$\hat{s}(x|\omega) = \frac{\hat{F}_{\mathrm{drive}}(x|\omega) L^4}{EI}. \tag{11}$$

The elastic properties of the cantilever beam can be implicitly removed from Eq. (10) by noting that the fundamental radial resonant frequency of the beam in vacuum, $\omega_{\mathrm{vac},1}$, is given by

$$\omega_{\mathrm{vac},1} = \frac{C_1^2}{L^2} \sqrt{\frac{EI}{\mu}}, \tag{12}$$

where $C_1 = 1.875104...$ is the smallest positive root of

$$1 + \cos C_n \cosh C_n = 0, \tag{13}$$

where $n=1,2,3,\ldots$. Substituting Eq. (12) into (10) then gives

$$\frac{d^4\hat{W}(x|\omega)}{dx^4}-B^4(\omega)\hat{W}(x|\omega)=\hat{s}(x|\omega), \tag{14}$$

where

$$B(\omega)=C_1\sqrt{\frac{\omega}{\omega_{\mathrm{vac},1}}}\left(1+\frac{\pi\rho b^2}{4\mu}\Gamma(\omega)\right)^{1/4}. \tag{15}$$

Since $\hat{s}(x|\omega)$ is taken to be arbitrary in this general formulation, it is convenient to express the solution of Eq. (14) in integral form, using the theory of Green's functions.[38] The appropriate Green's function $G(x,x'|\omega)$ for Eq. (14) satisfies

$$\frac{\partial^4 G(x,x'|\omega)}{\partial x^4}-B^4(\omega)G(x,x'|\omega)=\delta(x-x'), \tag{16}$$

where $\delta(x-x')$ is the Dirac delta function. The boundary conditions for Eq. (16) are identical to those presented in Eqs. (4). The solution of Eq. (16) for $G(x,x'|\omega)$ is given in Eq. (A4) of the Appendix A. From Eqs. (4), (14), and (16) it can then be easily shown[38] that the general solution to Eq. (14) is given by

$$\hat{W}(x|\omega)=\int_0^1 G(x,x'|\omega)\hat{s}(x'|\omega)dx'. \tag{17}$$

Equation (17) is the result we seek and gives the deflection function $\hat{W}(x|\omega)$ of the cantilever beam immersed in a viscous fluid as a function of an arbitrary normalized external driving force $\hat{s}(x|\omega)$. If the deflection function $w(x,t)$ in the time domain were required, then it could be obtained by taking the inverse Fourier transform of Eq. (17). However, this shall not be implemented in the present work, since we are primarily interested in the frequency response of the cantilever beam.

B. Hydrodynamic function $\Gamma(\omega)$ for circular and rectangular beams

We now present analytical expressions for the hydrodynamic functions $\Gamma(\omega)$ of beams that are circular and rectangular in cross section. For the rectangular cross section, it is assumed that the width b of the beam greatly exceeds its thickness h (see Fig. 2). As noted above, $\Gamma(\omega)$ is obtained by considering the rigid transverse oscillations of an infinitely long beam whose cross section is identical to that of the cantilever beam in question.

For a beam that is circular in cross section, the exact analytical result for $\Gamma(\omega)$ is well known,[39,40] and is given by

$$\Gamma_{\mathrm{circ}}(\omega)=1+\frac{4i\,K_1(-i\sqrt{i\,\mathrm{Re}})}{\sqrt{i\,\mathrm{Re}}\,K_0(-i\sqrt{i\,\mathrm{Re}})}, \tag{18}$$

where $\mathrm{Re}=\rho\omega b^2/(4\eta)$, as defined in Eq. (2), whereas b is the diameter of the cylinder and corresponds to the dominant length scale in the hydrodynamic flow, as discussed above. The subscript circ indicates that the solution refers to a circular cylinder. The functions K_0 and K_1 are modified Bessel functions of the third kind.[41]

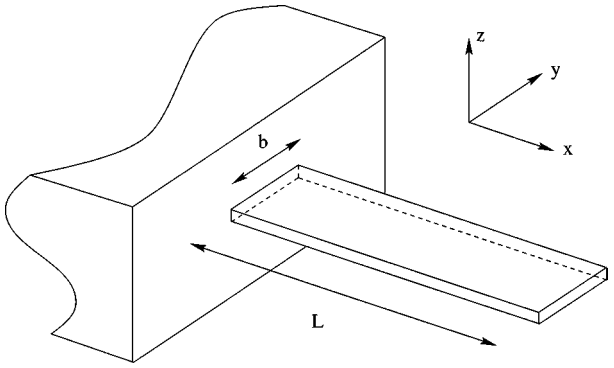

FIG. 2. Figure of rectangular beam showing dimensions. Thickness of beam is h. The origin of the coordinate system is at the center of mass of the cross section of the beam, at its clamped end.

In contrast, the formulation of an exact analytical solution to $\Gamma(\omega)$ for a beam that is rectangular in cross section poses a formidable challenge, and to our knowledge no such solution has appeared in the literature. However, the formulation can be greatly simplified by noting from the outset that the hydrodynamic function $\Gamma(\omega)$ of a rectangular beam of finite thickness is well approximated by that of an infinitely thin beam, provided its width b greatly exceeds its thickness h (see Fig. 2). An exact analytical solution to the latter problem was derived by Kanwal,[42] who formally expanded the governing equation for the stream function in elliptic coordinates, and consequently obtained a solution in terms of an infinite series in Mathieu functions.[41] Unfortunately, the resulting formulation is complicated and requires a significant amount of numerical computation. Therefore, we do not implement that solution, but instead refer to the more recent numerical and asymptotic investigations of Tuck,[43] who demonstrated that the hydrodynamic functions for a circular cylinder and an infinitely thin rectangular beam are approximately identical (deviations between the results never exceed 15% over the range $0.1\leqslant\mathrm{Re}\leqslant1000$).[43] Furthermore, from Appendix 1 of Ref. 43 it is evident that the hydrodynamic functions for a circular cylinder and a rectangular beam possess the same asymptotic forms in the limits as $\mathrm{Re}\to0$ and $\mathrm{Re}\to\infty$, namely,

$$\Gamma(\omega)=\begin{cases}1 & :\mathrm{Re}\to\infty\\ \dfrac{-4i}{\mathrm{Re}\,\ln(-i\sqrt{i\,\mathrm{Re}})} & :\mathrm{Re}\to0\end{cases}. \tag{19}$$

Consequently, it is a simple matter to formulate an approximate empirical correction function for Eq. (18) by interpolating the ratio of the results for the rectangular beam (obtained using the numerical procedure given in Ref. 43) with the results of Eq. (18). The hydrodynamic function for the rectangular beam $\Gamma_{\mathrm{rect}}(\omega)$ can then be expressed as

$$\Gamma_{\mathrm{rect}}(\omega)=\Omega(\omega)\Gamma_{\mathrm{circ}}(\omega), \tag{20}$$

where $\Omega(\omega)$ is the correction function, which shall now be evaluated. To perform the abovementioned interpolation, $\Omega(\omega)$ is expressed as a rational function in $\log_{10}\mathrm{Re}$, which satisfies the asymptotic conditions $\Omega(\omega)\to1$ as $\mathrm{Re}\to0$ and $\mathrm{Re}\to\infty$. The unknown coefficients in the rational function are

then evaluated by performing a nonlinear least-squares fit with the numerical data over the range $\mathrm{Re}\in[10^{-6},10^{4}]$. This procedure results in the following expressions for the real and imaginary parts of $\Omega(\omega)$,

$$\begin{aligned}\Omega_r(\omega)=&(0.91324-0.48274\tau+0.46842\tau^2-0.12886\tau^3\\&+0.044055\tau^4-0.0035117\tau^5+0.00069085\tau^6)\\&\times(1-0.56964\tau+0.48690\tau^2-0.13444\tau^3\\&+0.045155\tau^4-0.0035862\tau^5\\&+0.00069085\tau^6)^{-1},\end{aligned}\tag{21a}$$

$$\begin{aligned}\Omega_i(\omega)=&(-0.024134-0.029256\tau+0.016294\tau^2\\&-0.00010961\tau^3+0.000064577\tau^4\\&-0.000044510\tau^5)(1-0.59702\tau+0.55182\tau^2\\&-0.18357\tau^3+0.079156\tau^4-0.014369\tau^5\\&+0.0028361\tau^6)^{-1},\end{aligned}\tag{21b}$$

$$\tau=\log_{10}\mathrm{Re},\tag{22}$$

where $\Omega(\omega)=\Omega_r(\omega)+i\Omega_i(\omega)$. We emphasize that the resulting expression for $\Gamma_{\mathrm{rect}}(\omega)$, Eq. (20), is approximate in nature. Nonetheless, it is accurate to within 0.1% over the entire range $\mathrm{Re}\in[10^{-6},10^{4}]$ for both real and imaginary parts, and possesses the correct asymptotic forms as $\mathrm{Re}\to 0$ and $\mathrm{Re}\to\infty$. In the absence of any simple exact analytical formula for the hydrodynamic function of an infinitely thin rectangular beam, we use Eq. (20) in our present formulation.

Finally, we note that the hydrodynamic function $\Gamma(\omega)$ for a cantilever beam of arbitrary cross section can be numerically evaluated using the formulation given in Ref. 43.

C. Frequency response due to a thermal driving force

In this section, we apply the present formulation to the analysis of the frequency response of a cantilever beam that is excited thermally, i.e., by Brownian motion of the molecules in the surrounding fluid. Any dissipative effects due to internal frictional losses in the beam are assumed to be negligible in comparison to those exhibited by the fluid. Since these conditions are typically satisfied in AFM cantilever beams,[5,28,32] the results to be presented in this section directly give the thermal noise spectra of these cantilevers.

Since the cantilever beam is excited by Brownian motion of the molecules in the fluid, it is clear that the external driving force being applied to the beam is uncorrelated in position and is stochastic in nature. It then directly follows that the Fourier transform of this driving force $\hat{F}_{\mathrm{drive}}(x|\omega)$ is independent of position x along the beam, i.e.,

$$\hat{F}_{\mathrm{drive}}(x|\omega)=\hat{F}_{\mathrm{drive}}(\omega).\tag{23}$$

At this stage we note that the expectation value of the potential energy for each mode of the beam must be identically equal to the thermal energy $1/2k_BT$, where k_B is Boltzmann's constant and T is absolute temperature. Since this is the case, it then directly follows that stochastic forces exciting different modes of the beam also differ in magnitude. To evaluate the magnitudes of each of these driving forces, the modes of the damped cantilever beam must be decomposed into the modes of the undamped beam, since any damping will couple all modes. The undamped modes of a cantilever beam are given by

$$\begin{aligned}\phi_n(x)=&(\cos C_n x-\cosh C_n x)+\frac{\cos C_n+\cosh C_n}{\sin C_n+\sinh C_n}\\&\times(\sinh C_n x-\sin C_n x),\end{aligned}\tag{24}$$

where C_n is a solution to Eq. (13).

To decompose the deflection function of the damped cantilever beam into the modes of the undamped beam, we simply use the properties that (i) the modes $\phi_n(x)$ form an orthonormal basis set and (ii) each mode is excited by a stochastic driving force whose magnitude is dictated by the above energy criterion. It then follows (see Appendix B) that the deflection function of the cantilever beam $\hat{W}(x|\omega)$ can be expressed as

$$\hat{W}(x|\omega)=\sum_{n=1}^{\infty}\hat{F}_n(\omega)\alpha_n(\omega)\phi_n(x),\tag{25}$$

where

$$\alpha_n(\omega)=\frac{2\sin C_n\tan C_n}{C_n(C_n^4-B^4(\omega))(\sin C_n+\sinh C_n)},\tag{26}$$

$$|\hat{F}_n(\omega)|_s^2=\frac{3\pi k_BT}{kC_n^4\int_0^{\infty}|\alpha_n(\omega')|^2d\omega'},\tag{27}$$

where the subscript s refers to the spectral density, $B(\omega)$ is defined in Eq. (15), and the spring constant of the beam k is given by

$$k=\frac{3EI}{L^3}.\tag{28}$$

Substituting Eq. (27) into (25) and noting that all modes are uncorrelated, we obtain the required results

$$|\hat{W}(x|\omega)|_s^2=\frac{3\pi k_BT}{k}\sum_{n=1}^{\infty}\frac{|\alpha_n(\omega)|^2}{C_n^4\int_0^{\infty}|\alpha_n(\omega')|^2d\omega'}\phi_n^2(x),\tag{29a}$$

$$\begin{aligned}\left|\frac{\partial\hat{W}(x|\omega)}{\partial x}\right|_s^2=&\frac{3\pi k_BT}{k}\sum_{n=1}^{\infty}\frac{|\alpha_n(\omega)|^2}{C_n^4\int_0^{\infty}|\alpha_n(\omega')|^2d\omega'}\\&\times\left(\frac{d\phi_n(x)}{dx}\right)^2.\end{aligned}\tag{29b}$$

For a detailed derivation of the above results, the reader is referred to Appendix B.

Equation (29a) gives the frequency response of the square of the magnitude of the displacement function at all positions along the beam, whereas Eq. (29b) gives the corresponding result for the slope. We note that in AFM applications, the magnitude of the slope is typically measured [i.e., square root of Eq. (29b)], since deflections of the beam are often obtained using optical detection systems. Equations

(29a) and (29b) then give the relationship between the frequency spectra of the slope and displacement of the beam.

Finally, we note that the total thermal noise present in each mode of the frequency response of the beam, which is obtained by integrating Eq. (29a) or (29b) over all frequencies, is independent of the damping in the system. Consequently, these results indicate that the analysis presented by Butt *et al.*,[30] for the total thermal noise in all modes of an undamped cantilever beam, also applies to cantilever beams with arbitrary damping.

D. Limit of small dissipative effects

We now examine the special case where dissipative effects in the fluid can be considered to be small, i.e., when the magnitude of the imaginary component of $B(\omega)$ is far smaller than that of its real component. In particular, we consider in detail the case of a cantilever beam excited by a thermal driving force, for which explicit general results for the frequency response of the beam are given in the preceding section. As a result, we demonstrate that the frequency response of each mode of the beam is well approximated by that of a SHO in this limit, and consequently give explicit expressions for the resonant frequency and quality factor of the beam.

To begin, we note that in the limit of small dissipative effects, the modes of the beam are weakly coupled, and consequently can be considered to be uncoupled, to leading order. It then directly follows from Eq. (29a) that the magnitude of $\hat{W}(x|\omega)$ in the neighborhood of the resonance peak of mode n is well approximated by

$$|\hat{W}(x|\omega)|_s \cong \left| \frac{a_n(x)}{C_n^4 - B^4(\omega)} \right|, \tag{30}$$

where the function $a_n(x)$ is independent of frequency ω and is given by

$$a_n(x) = \left\{ \frac{12\pi k_B T \sin^2 C_n \tan^2 C_n}{k C_n^6 (\sin C_n + \sinh C_n)^2 \int_0^\infty |\alpha_n(\omega')|^2 d\omega'} \right\}^{1/2} \times \phi_n(x). \tag{31}$$

We note that Eq. (30) also holds for the frequency response of the slope of the beam Eq. (29b), except that the function $a_n(x)$ is modified accordingly.

Since $B(\omega)$ has a small imaginary component in these cases, it is clear from Eq. (30) that the resonance peaks will be sharp yet finite it nature. Furthermore, from Eqs. (15) and (18) it is evident that in the neighborhood of a resonance peak, variations in $B^4(\omega)$ are dominated by an $O(\omega^2)$ contribution, since the hydrodynamic function $\Gamma(\omega)$ varies slowly as $O(\omega^{-1/2})$.[39] Consequently, in the neighborhood of the resonance peak of mode n, $\Gamma(\omega)$ can be considered to be constant, to leading order, and evaluated at the resonance frequency of the mode in the absence of dissipative effects, $\omega_{R,n}$. Generalizing Eq. (15) to encompass all modes, we then find that in the neighborhood of the resonance peak of mode n, $B(\omega)$ is well approximated by

$$B(\omega) \cong B_n(\omega) = C_n \sqrt{\frac{\omega}{\omega_{\text{vac},n}}} \left[1 + \frac{\pi \rho b^2}{4\mu} (\Gamma_r(\omega_{R,n}) + i\Gamma_i(\omega_{R,n})) \right]^{1/4}, \tag{32}$$

where $\omega_{\text{vac},n}$ is the resonant frequency in vacuum of mode n, whereas Γ_r and Γ_i are the real and imaginary components of $\Gamma(\omega)$, respectively. From Eq. (32), it is also clear that the resonant frequency of mode n in the absence of dissipative effects, $\omega_{R,n}$, is given by

$$\frac{\omega_{R,n}}{\omega_{\text{vac},n}} = \left(1 + \frac{\pi \rho b^2}{4\mu} \Gamma_r(\omega_{R,n}) \right)^{-1/2}. \tag{33}$$

Substituting Eq. (33) into (32) and rearranging we find that $B_n(\omega)$ becomes

$$B_n(\omega) = C_n \sqrt{\frac{\omega}{\omega_{R,n}}} \left(1 + \frac{i}{Q_n} \right)^{1/4}, \tag{34}$$

where

$$Q_n = \frac{\frac{4\mu}{\pi \rho b^2} + \Gamma_r(\omega_{R,n})}{\Gamma_i(\omega_{R,n})}. \tag{35}$$

Substituting Eq. (34) into (30), and noting that in the limit of small dissipative effects, $\omega \cong \omega_{R,n}$, we then find

$$\left| \frac{C_n^4 \hat{W}(x|\omega)}{a_n(x) \omega_{R,n}^2} \right|_s \cong \left[(\omega^2 - \omega_{R,n}^2)^2 + \frac{\omega^2 \omega_{R,n}^2}{Q_n^2} \right]^{-1/2}, \tag{36}$$

which is immediately identifiable as the frequency response of a SHO, with resonant frequency $\omega_{R,n}$ and quality factor Q_n defined in Eqs. (33) and (35), respectively. We emphasize that the above conclusions and formulae for the resonant frequency and quality factor also hold for the frequency response of the slope of the beam.

Finally we note that if $Q_n \gg 1$, it is clear from Eq. (34) that dissipative effects in the fluid can be considered to be small, and the analogy with the SHO is valid. Conversely, if $Q_n \lesssim O(1)$, then it is evident that such an analogy is not justified. We shall examine these two cases in detail in the following sections.

IV. RESULTS AND DISCUSSION

Results shall now be be presented for the frequency response of cantilever beams of *rectangular* cross section that are excited thermally; see Fig. 2. Throughout, it is assumed that the width b of the beam greatly exceeds its thickness h; the hydrodynamic function $\Gamma(\omega)$ is defined in Eq. (20). This case is considered in detail since it is of significant practical importance in application to the AFM. We emphasize, however, that the general formulation presented is applicable to beams of arbitrary cross section that are excited by arbitrary driving forces.

To begin we note that the present theoretical model approximates the hydrodynamic flow around a cantilever beam of large but finite aspect ratio by one that is infinite in aspect ratio. Therefore, it is clear that the model is applicable in

practice provided the mode number n is not large (i.e., the fundamental mode and its first few harmonics). Consequently, we shall primarily restrict our discussion to the fundamental mode and in some instances examine the effects on the higher order modes.

We now define the scaling parameters for the problem which will enable us to examine the frequency response of cantilever beams of arbitrary dimensions and material properties, immersed in viscous fluids of arbitrary density and viscosity. From Eqs. (15) and (18), it is evident that the two natural scaling parameters $\overline{\mathrm{Re}}$ and $\overline{T}$ for the problem are

$$\overline{\mathrm{Re}}=\frac{\rho\omega_{\mathrm{vac},1}b^2}{4\eta},\quad \overline{T}=\frac{\rho b}{\rho_c h}, \tag{37}$$

where b is the width of the beam, h is its thickness, $\omega_{\mathrm{vac},1}$ is the radial resonant frequency of the fundamental mode of the beam in vacuum, and use has been made of the property that the mass per unit length of the beam $\mu=\rho_c bh$. The parameter $\overline{\mathrm{Re}}$ is a normalized Reynolds number that indicates the importance of viscous forces relative to inertial forces in the fluid. In contrast, $\overline{T}$ is proportional to the ratio of the added-apparent mass due to inertial forces in the fluid (in the absence of viscous effects), to the total mass of the beam. Furthermore, from Eqs. (12) and (37) it is evident that the parameter $\overline{\mathrm{Re}}$ can be expressed explicitly in terms of the geometric and material properties of the beam

$$\overline{\mathrm{Re}}=\frac{C_1^2}{8\sqrt{3}}\,h\left(\frac{b}{L}\right)^2\frac{\rho}{\eta}\sqrt{\frac{E}{\rho_c}}. \tag{38}$$

From Eqs. (37) and (38) it is then clear that as the dimensions of the cantilever beam are ''uniformly'' reduced, $\overline{T}$ remains unchanged whereas the Reynolds number $\overline{\mathrm{Re}}$ decreases linearly with the thickness h. We shall examine the implications of this decrease in $\overline{\mathrm{Re}}$ with decreasing beam size (i.e., at constant $\overline{T}$) in the following discussion.

Before presenting the results, we note that values of $\overline{T}$ for beams immersed in gases and liquids typically differ by three orders of magnitude. This is a direct result of the difference in densities of gases relative to those of liquids. In contrast, values for $\overline{\mathrm{Re}}$ in gases and liquids differ by only one order of magnitude, since the kinematic viscosities η/ρ of gases are typically one order of magnitude greater than those of liquids. Consequently, we shall present separate results for gases and liquids that account for these differences.

In the limit of vanishing viscous effects, $\overline{\mathrm{Re}}\to\infty$, we find from Eqs. (19) and (33) that the resonant frequencies of the beam, $\omega_{R,n}$ are given explicitly in terms of its frequencies in vacuum, $\omega_{\mathrm{vac},n}$, namely

$$\frac{\omega_{R,n}}{\omega_{\mathrm{vac},n}}=\left(1+\frac{\pi\rho b}{4\rho_c h}\right)^{-1/2}, \tag{39}$$

which is the well-known result due to Chu.[1] We shall use Eq. (39) as our benchmark to examine the effects of viscosity on the frequency response of cantilever beams immersed in viscous fluids.

In Fig. 3 we present results for the frequency response of the slope at the end point ($x=1$) of cantilever beams immersed in gases, for various values of $\overline{\mathrm{Re}}$ and $\overline{T}$. Results are given for $\overline{\mathrm{Re}}\sim O(1)$ and $\overline{T}\sim O(10^{-2})$, since these correspond to values typically encountered in practice.[18,23,28] In all cases, only the region in the neighborhood of the fundamental resonance peak is shown. Also indicated is the quality factor Q_1 of each resonance peak, as evaluated from Eq. (35), and the resonant frequency in the limit as $\overline{\mathrm{Re}}\to\infty$, Eq. (39). It is evident from Fig. 3 that for a given value of $\overline{T}$, decreasing $\overline{\mathrm{Re}}$ broadens and shifts the resonance peaks to lower frequencies, a direct result of the increasing importance of viscous effects in the fluid. Furthermore, we note that the peak frequencies are significantly lower than those predicted by the inviscid fluid model, Eq. (39), for all cases considered. We emphasize that the shift in the peak frequency is primarily accounted for by Eq. (33), which neglects any dissipative effects, indicating that an increase in inertial forces is the primary cause. These results are consistent with recent experimental results of AFM cantilevers,[17] where it was demonstrated that the shift in the resonant frequency from vacuum to air cannot be account for by the broadening of the resonance peak or by the inviscid fluid model, Eq. (39). A comparison of such experimental and theoretical results shall be deferred to Ref. 33, where a detailed study shall be pre-

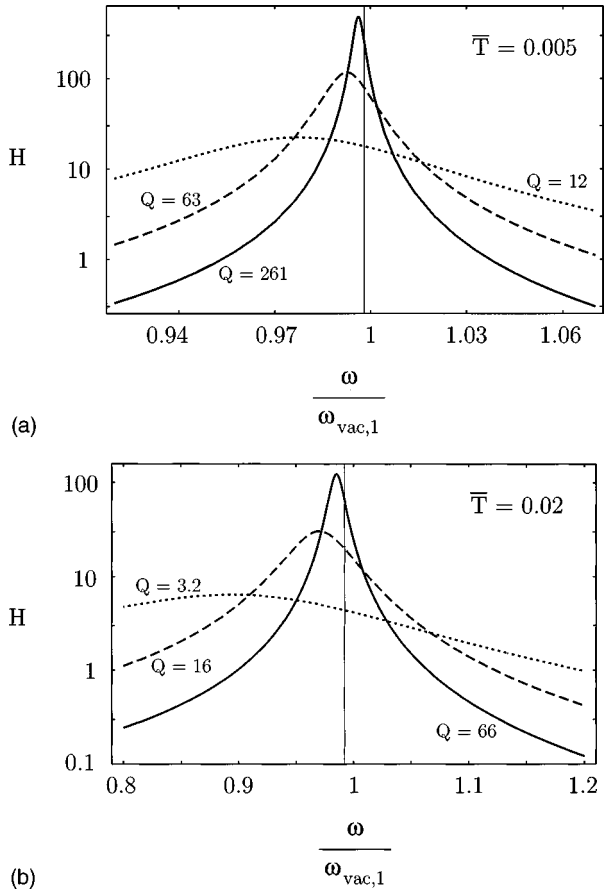

FIG. 3. Normalized thermal spectra $H\equiv|\hat{W}'(1|\omega)|_s^2 k\omega_{\mathrm{vac},1}/(2k_BT)$, Eq. (29b), of fundamental mode in neighborhood of peak. The $'$ refers to the derivative with respect to x. Frequencies obtained using the inviscid formula Eq. (39) are indicated by vertical lines. Quality factor $Q\equiv Q_1$, Eq. (35), is indicated for each case. $\overline{\mathrm{Re}}=0.1$ (short-dashed line); $\overline{\mathrm{Re}}=1$ (dashed line); $\overline{\mathrm{Re}}=10$ (solid line). (a) $\overline{T}=0.005$; (b) $\overline{T}=0.02$.

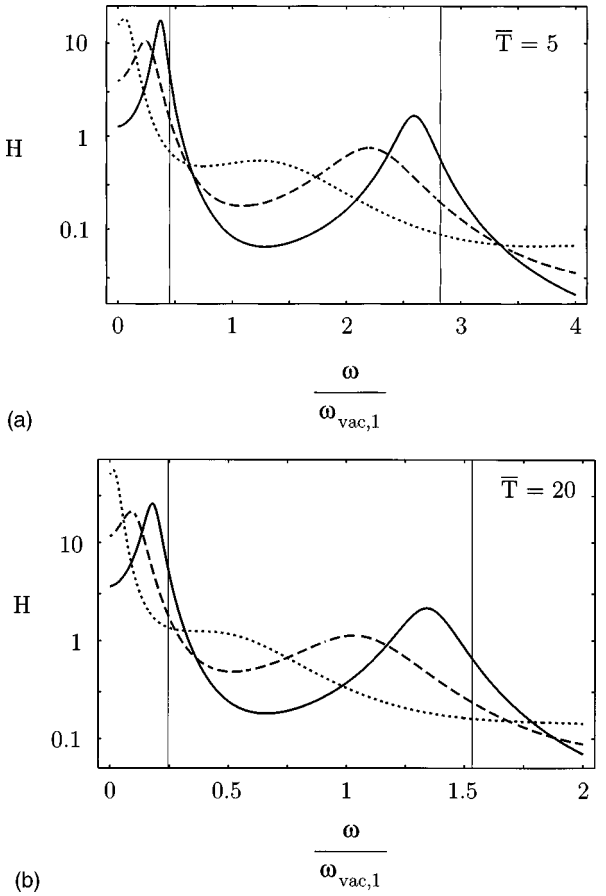

FIG. 4. Normalized thermal spectra $H \equiv |\hat{W}'(1|\omega)|_s^2 k\omega_{vac,1}/(2k_BT)$, Eq. (29b), displaying fundamental mode and its first harmonic. The $'$ refers to the derivative with respect to x. Frequencies obtained using the inviscid formula Eq. (39) are indicated by vertical lines. $\overline{Re}=1$ (short-dashed line); $\overline{Re}=10$ (dashed line); $\overline{Re}=100$ (solid line). (a) $\overline{T}=5$; (b) $\overline{T}=20$.

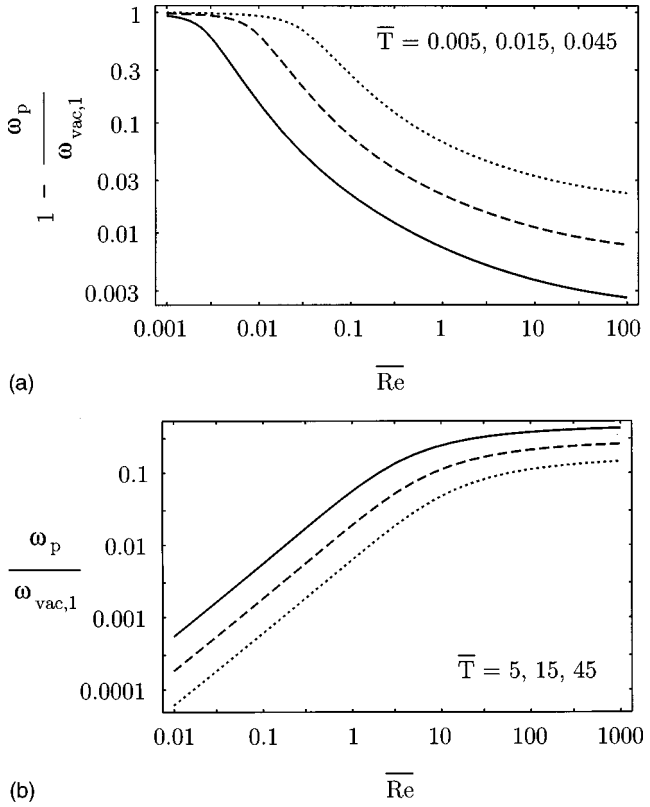

FIG. 5. Plot of peak frequency ω_p of fundamental resonance relative to frequency in vacuum $\omega_{vac,1}$. (a) $\overline{T}=0.045$ (short-dashed line); $\overline{T}=0.015$ (dashed line); $\overline{T}=0.005$ (solid line). Results in the limit $\overline{Re}\to\infty$ for $\overline{T}=0.045$, 0.015, 0.005 are $(1-\omega_p/\omega_{vac,1})=0.0172$, 0.00584, 0.00196, respectively. (b) $\overline{T}=45$ (short-dashed line); $\overline{T}=15$ (dashed line); $\overline{T}=5$ (solid line); Results in the limit $\overline{Re}\to\infty$ for $\overline{T}=45$, 15, 5 are $\omega_p/\omega_{vac,1}=0.166$, 0.280, 0.451, respectively.

sented. The results in Fig. 3 also demonstrate that for a given $\overline{Re}$, an increase in $\overline{T}$ has the effect of broadening and shifting the resonance peak to lower frequencies. Again, this is a direct result of an increase in viscous effects in the fluid.

In Fig. 4 we give analogous results for cantilever beams immersed in liquids. In this case, the frequency response includes the fundamental mode and its first harmonic and results are presented for $\overline{T}\sim O(10)$ and $\overline{Re}\sim O(10)$. These values for $\overline{Re}$ and $\overline{T}$ are chosen since they correspond to typical practical values for AFM cantilever beams immersed in liquids.[14,18,23] Note the dramatic shifting and broadening in the fundamental resonance peak compared to the results presented in Fig. 3 for gases. It is also clear that significant coupling occurs between the fundamental mode and its first harmonic. In some cases, the first harmonic resonance peak has almost vanished and the peak in the fundamental mode is very close to zero frequency, due to the dramatic effect of the surrounding fluid. In all cases note that the peak frequencies of both the fundamental mode and its first harmonic occur at significantly lower frequencies than that predicted by the inviscid fluid model, Eq. (39). Furthermore, we note that the general trends regarding variations in $\overline{Re}$ and $\overline{T}$ discussed above also apply to the results presented in Fig. 4.

To quantify the general trends discussed above, in Figs. 5 and 6 we present detailed results for the peak frequency ω_p and quality factor Q_1 of the fundamental resonance, as a function of both $\overline{Re}$ and $\overline{T}$. The peak frequency is numerically calculated from the frequency response, Eq. (29b), whereas the quality factor is obtained directly from Eq. (35). Consequently, results presented for Q_1 give quantitative information about the resonance peak provided $Q_1 \gg 1$, since the analogy with the frequency response of a SHO is only valid in those cases. For $Q_1 \lesssim O(1)$, however, no such analogy exists and Q_1 only presents qualitative information about the resonance peak. In particular, for $Q_1 \lesssim O(1)$ one can conclude that substantial broadening of the resonance peak is present, and that the modes are significantly coupled. A reduction in Q_1 will then result in further broadening of the peak and an increased coupling of the modes. Finally, it is interesting to note that a nonzero peak frequency is observed in all cases presented. Such behavior is not observed in a SHO model, where the peak frequency is found to be identically zero for all quality factors $Q_1 \leqslant 1/\sqrt{2}$. These results demonstrate that for $Q_1 \lesssim O(1)$ the frequency response of a cantilever beam is not analogous to that of a SHO. We shall discuss this in more detail below.

Of particular interest in application to the AFM is the peak energy of the fundamental resonance, since this is observed as noise in measurements made using the AFM.[18] In

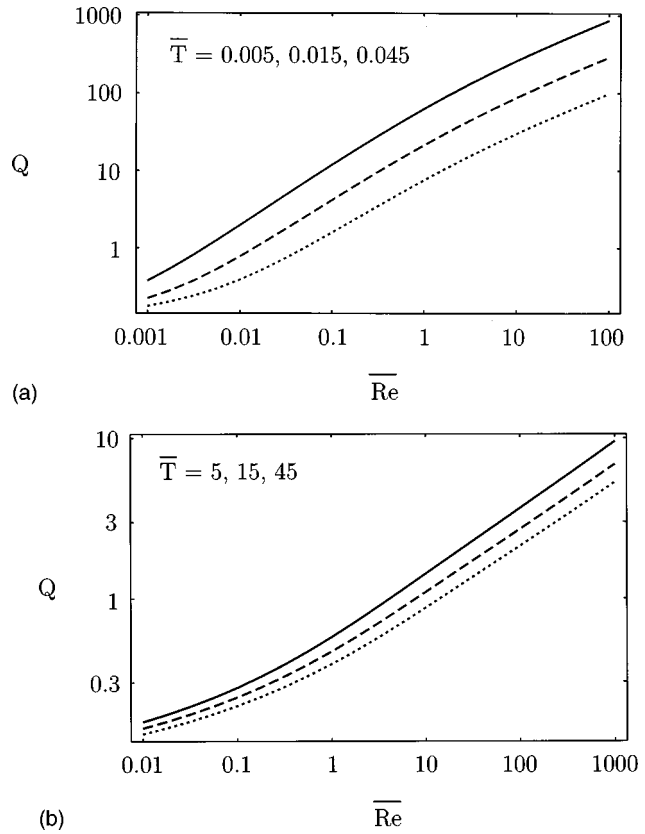

FIG. 6. Plot of quality factor $Q \equiv Q_1$, Eq. (35), for the fundamental mode. (a) $\overline{T}=0.045$ (short-dashed line); $\overline{T}=0.015$ (dashed line); $\overline{T}=0.005$ (solid line). (b) $\overline{T}=45$ (short-dashed line); $\overline{T}=15$ (dashed line); $\overline{T}=5$ (solid line);

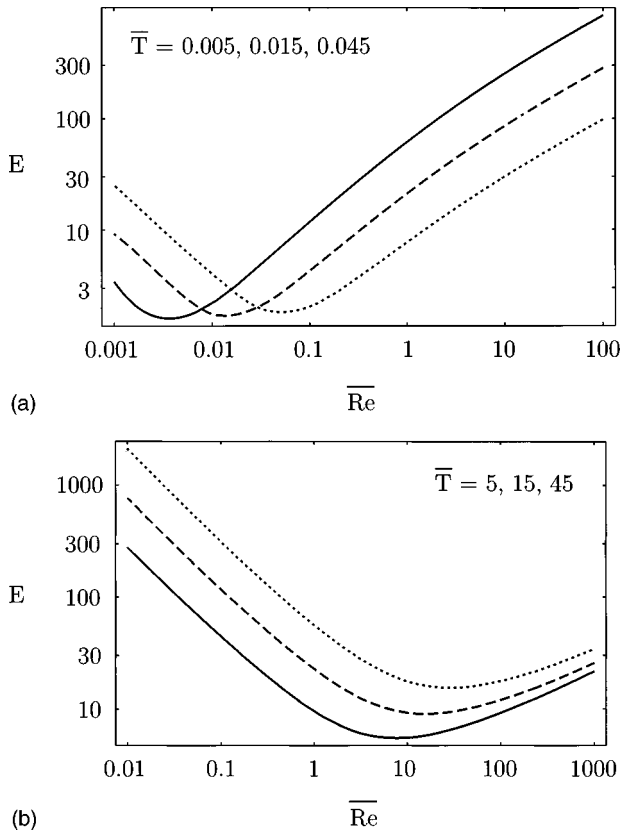

FIG. 7. Plot of normalized peak energy of fundamental resonance $E \equiv |\hat{W}(1|\omega)|_s^2 k \omega_{\mathrm{vac},1}/(2k_B T)$ as obtained from Eq. (29a). (a) $\overline{T}=0.045$ (short-dashed line); $\overline{T}=0.015$ (dashed line); $\overline{T}=0.005$ (solid line). (b) $\overline{T}=45$ (short-dashed line); $\overline{T}=15$ (dashed line); $\overline{T}=5$ (solid line);

Fig. 7 we present the normalized peak energy of the fundamental resonance for gases and liquids, respectively; all results were obtained numerically from Eq. (29a). Note that in all cases examined, the normalized peak energy displays a minimum at a critical value $\overline{\mathrm{Re}}_{\mathrm{min}}$ as the scaled Reynolds number $\overline{\mathrm{Re}}$ is varied for a given $\overline{T}$. Consequently, for $\overline{\mathrm{Re}} > \overline{\mathrm{Re}}_{\mathrm{min}}$ this peak energy increases monotonically with increasing $\overline{\mathrm{Re}}$, whereas for $\overline{\mathrm{Re}} < \overline{\mathrm{Re}}_{\mathrm{min}}$ it increases with decreasing $\overline{\mathrm{Re}}$. Upon comparison of Figs. 6(a), 7(a) and Figs. 6(b), 7(b) it is evident that $\overline{\mathrm{Re}}_{\mathrm{min}}$ also corresponds to the value of $\overline{\mathrm{Re}}$ where $Q_1 \sim 1$, indicating that dissipative effects can be considered to be small for $\overline{\mathrm{Re}} > \overline{\mathrm{Re}}_{\mathrm{min}}$ and significant for $\overline{\mathrm{Re}} < \overline{\mathrm{Re}}_{\mathrm{min}}$. Since the energy in any one mode is fixed, it follows that if dissipative effects are small, then all modes are weakly coupled and the normalized peak energy will decrease with decreasing $\overline{\mathrm{Re}}$, due to the redistribution of the energy over a larger frequency range, as observed for $\overline{\mathrm{Re}} > \overline{\mathrm{Re}}_{\mathrm{min}}$. However, if dissipative effects in the fluid are significant, we find that the energy in the fundamental mode redistributes itself towards lower frequencies (see Fig. 4), resulting in an increase in the peak energy for decreasing $\overline{\mathrm{Re}}$, as observed for $\overline{\mathrm{Re}} < \overline{\mathrm{Re}}_{\mathrm{min}}$. We emphasize that this increase in peak energy is not due to coupling of the higher order modes into the fundamental mode, since this always remains minimal, as we shall demonstrate below. These results then indicate the possibility that the peak energy observed for a given cantilever beam in air can in fact be smaller than that observed for the same cantilever immersed in water. This phenomenon depends of course on the specific values of $\overline{\mathrm{Re}}$ and $\overline{T}$ of the cantilever in question, as is evident from Fig. 7.

Next we examine the influence of the surrounding fluid on the magnitude of the deflection functions of the modes, henceforth referred to as the mode shapes, at their peak resonant frequencies. In particular, we study the fundamental mode and its first two harmonics, which correspond to modes 1, 2, and 3, respectively. In Fig. 8(a) we give the mode shapes of the fundamental mode for various values of $\overline{\mathrm{Re}}$ and for a fixed value of $\overline{T}=5$. Also included in Fig. 8(a) is the mode shape in the absence of viscous effects ($\overline{\mathrm{Re}} \to \infty$), which corresponds to no mode coupling. It is strikingly evident from Fig. 8(a) that the mode shape of the fundamental mode at peak frequency is virtually unaffected by the presence of dissipative effects in the fluid, demonstrating that coupling of higher order modes into the fundamental mode is insignificant. In contrast to the fundamental mode, we observe in Fig. 8(b) and 8(c) that its first and second harmonics, modes 2 and 3, are both strongly affected by the presence of dissipative effects in the fluid. Unlike the mode shapes in the absence of viscous effects, it is clear that the nodes in the deflection function are eliminated by the fluid, a direct consequence of the strong coupling between modes when dissipative effects in the fluid are significant.

In Sec. III D we rigorously showed that the frequency response of a cantilever beam is identical to that of a SHO,

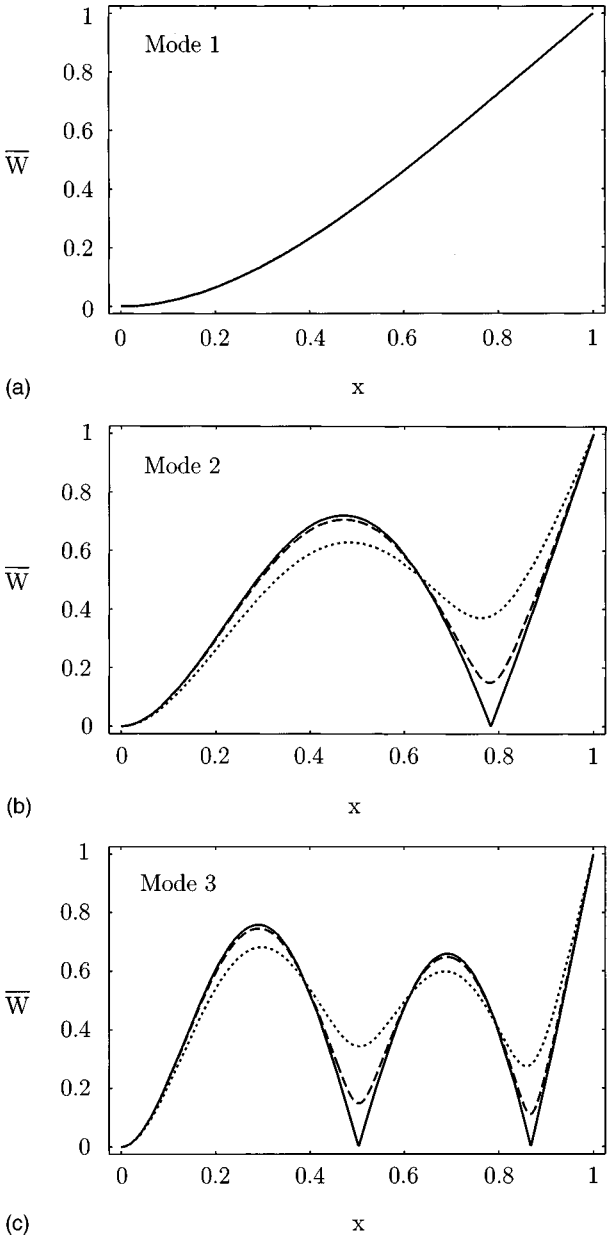

FIG. 8. Comparison of normalized mode shapes $\overline{W} \equiv |\hat{W}(x|\omega_p)|_s / |\hat{W}(1|\omega_p)|_s$ at the peak resonant frequencies of each mode for $\overline{T}=5$. $\overline{\mathrm{Re}}=1$ (short-dashed line); $\overline{\mathrm{Re}}=10$ (dashed line); $\overline{\mathrm{Re}}\to\infty$ (solid line). (a) Mode 1; (b) Mode 2; (c) Mode 3.

provided dissipative effects in the fluid can be considered to be small, i.e., $Q_n \gg 1$. We now demonstrate that this analogy is not valid for cases where dissipative effects are not small, i.e., $Q_n \lesssim O(1)$. In Fig. 9 we present the frequency response obtained from Eq. (29a) for the case where $\overline{\mathrm{Re}}=10$, $\overline{T}=15$, in the neighborhood of the fundamental mode, for which $Q_1 \cong 1$. We found that for the values of $\overline{\mathrm{Re}}$ and $\overline{T}$ chosen, the frequency response over the entire frequency range indicated was virtually unaffected by the presence of the higher order modes, in line with the results presented above. Also shown in Fig. 9 is the frequency response of a SHO, whose resonant frequency and quality factor were chosen to ensure that the fit in the neighborhood of the true resonant peak was optimal. This was achieved by performing a nonlinear least-

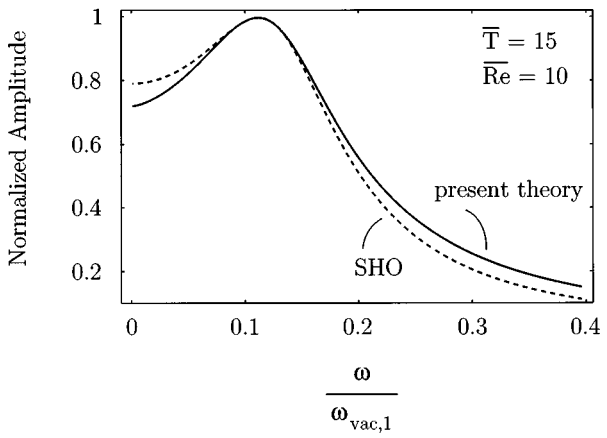

FIG. 9. Comparison of amplitude frequency response of fundamental mode evaluated using Eq. (29a) (solid line) to best fit of SHO response (dashed line) for $\overline{T}=15$ and $\overline{\mathrm{Re}}=10$. Peak amplitude of response is normalized to unity.

squares fit of the SHO model to the results of Eq. (29a). From Fig. 9 it is clear that the frequency response of a SHO is a poor approximation to the true frequency response of the cantilever beam in this case.

V. CONCLUSIONS

We have presented a general theoretical model for the frequency response of a cantilever beam of arbitrary cross section, immersed in a viscous fluid and excited by an arbitrary driving force. The primary restrictions of this model are that the length of the beam must greatly exceed its nominal width, the amplitude of vibration must be small, and the fluid must be incompressible in nature, properties that are satisfied in many cases of practical interest. Unlike previous formulations, the present model accounts for the loading induced by the viscous fluid in a rigorous and quantitative fashion, thus enabling the frequency response to be determined in an *a priori* manner from a knowledge of the material and geometric properties of the beam and the viscosity and density of the fluid. Since beams of circular or rectangular cross section are of significant importance in many applications, we also presented explicit analytical formulae for their corresponding hydrodynamic functions, which will facilitate the calculation of their frequency responses.

The response of a cantilever beam to a thermal driving force was considered in detail, due to its fundamental significance in application to the AFM. It was found that the importance of viscous effects is strongly dependent on the dimensions of the beam; decreasing these dimensions enhances viscous effects, resulting in increased broadening and shifting of the resonant peak from its value in vacuum. For the case where dissipative effects in the fluid can be considered to be small, it was shown that the frequency response of a cantilever beam is well approximated by that of a SHO in the neighborhood of a resonant peak, for which we presented explicit analytical expressions for the resonant frequency and quality factor. Finally, we presented detailed numerical results for the frequency response of rectangular cantilever beams of arbitrary dimensions, immersed in viscous fluids of

arbitrary properties, which we believe will be of significant practical value to the users and designers of AFM cantilever beams.

ACKNOWLEDGMENTS

The author would like to express his sincere gratitude to Dr. P. Mulvaney and J. W. M. Chon from the Department of Chemistry, University of Melbourne, Dr. J. P. Cleveland from Digital Instruments, USA, T. Schaeffer from the Department of Physics, University of California, Santa Barbara, and Professors D. Y. C. Chan and L. R. White from the Department of Mathematics and Statistics, University of Melbourne, for many interesting and stimulating discussions. This research was carried out with the support of Advanced Minerals Product Centre, an ARC Special Research Centre and was also supported in part by ARC Grant No. S69812864.

APPENDIX A

In this appendix, we derive the Green's function $G(x,x'|\omega)$ for the deflection of a cantilever beam. To begin, we note that the governing equation for $G(x,x'|\omega)$ is

$$\frac{\partial^4 G(x,x'|\omega)}{\partial x^4} - B^4(\omega) G(x,x'|\omega) = \delta(x-x'), \tag{A1}$$

where $\delta(x-x')$ is the Dirac delta function. The boundary conditions for $G(x,x'|\omega)$ at the clamped and free ends are identical to those of $\hat{W}(x|\omega)$, namely

$$\left[G(x,x'|\omega) = \frac{\partial G(x,x'|\omega)}{\partial x} \right]_{x=0}$$

$$= \left[\frac{\partial^2 G(x,x'|\omega)}{\partial x^2} = \frac{\partial^3 G(x,x'|\omega)}{\partial x^3} \right]_{x=1} = 0. \tag{A2}$$

In addition to these boundary conditions, it can be easily shown, upon integration of Eq. (A1), that $G(x,x'|\omega)$ also satisfies the following continuity conditions at $x=x'$,

$$\lim_{\epsilon \to 0^+} \left[\frac{\partial^3 G(x,x'|\omega)}{\partial x^3} \right]_{x=x'-\epsilon}^{x=x'+\epsilon} = 1, \tag{A3}$$

with $\partial^2 G/\partial x^2$, $\partial G/\partial x$, G all being continuous at $x=x'$.

The Green's function is then constructed in an analogous manner to Ref. 38, by applying the above boundary and continuity conditions to the general solution of the corresponding homogeneous equation [i.e., Eq. (A1) with the right hand side replace by zero], and making use of the symmetry property $G(x,x'|\omega) = G(x',x|\omega)$, from which we obtain

$$G(x,x'|\omega) = \frac{1}{4B^3(\omega)[1+\cos B(\omega)\cosh B(\omega)]} \begin{cases} ([\cos B(\omega)+\cosh B(\omega)][\cosh B(\omega)x - \cos B(\omega)x] \\ \quad +[\sin B(\omega)-\sinh B(\omega)][\sinh B(\omega)x - \sin B(\omega)x]) \\ \quad \times(\sin(B(\omega)[x'-1]) + \sinh(B(\omega)[x'-1])) \\ \quad +([\cos B(\omega)+\cosh B(\omega)][\sin B(\omega)x - \sinh B(\omega)x] \\ \quad -[\sin B(\omega)+\sinh B(\omega)][\cos B(\omega)x - \cosh B(\omega)x] \\ \quad \times(\cos(B(\omega)[x'-1]) + \cosh(B(\omega)[x'-1])) \quad : 0 \leqslant x \leqslant x' \leqslant 1 \\ ([\cos B(\omega)+\cosh B(\omega)][\cosh B(\omega)x' - \cos B(\omega)x'] \\ \quad +[\sin B(\omega)-\sinh B(\omega)][\sinh B(\omega)x' - \sin B(\omega)x'] \\ \quad \times(\sin(B(\omega)[x-1]) + \sinh(B(\omega)[x-1])) \\ \quad +([\cos B(\omega)+\cosh B(\omega)][\sin B(\omega)x' - \sinh B(\omega)x'] \\ \quad -[\sin B(\omega)+\sinh B(\omega)][\cos B(\omega)x' - \cosh B(\omega)x'] \\ \quad \times(\cos(B(\omega)[x-1]) + \cosh(B(\omega)[x-1])) \quad : 0 \leqslant x' \leqslant x \leqslant 1. \end{cases} \tag{A4}$$

APPENDIX B

In this appendix, we give the formal derivation of the results presented in Sec. III C for the frequency response of a cantilever beam excited by a thermal driving force.

To begin, we note that the deflection function $\hat{W}(x|\omega)$ of a cantilever beam with arbitrary damping can be decomposed into its individual undamped modes $\phi_n(x)$, defined in Eq. (24), by using the property that $\phi_n(x)$ form an orthonormal basis set, i.e.,

$$\int_0^1 \phi_i(x)\phi_j(x)dx = \begin{cases} 1 & : i=j \\ 0 & : \text{otherwise} \end{cases}. \tag{B1}$$

For the case of thermal excitation, each mode of the beam is driven by a stochastic force of different magnitude, as discussed in Sec. III C. Noting this, and using the above orthogonality property for $\phi_n(x)$, it then follows that the deflection function $\hat{W}(x|\omega)$ can be expressed as

$$\hat{W}(x|\omega) = \sum_{n=1}^{\infty} \hat{F}_n(\omega)\alpha_n(\omega)\phi_n(x), \tag{B2}$$

where

$$\alpha_n(\omega) = \int_0^1 \hat{W}_0(x|\omega)\phi_n(x)dx, \tag{B3}$$

where $\hat{F}_n(\omega)$ is the stochastic driving force for mode n. The function $\hat{W}_0(x|\omega)$ is the ''transfer function'' of the cantilever beam and is given by its deflection function due to a uniform impulse driving force applied along its entire length, i.e., $\hat{F}_{\text{drive}}(\omega)=1$. From Eq. (17) it then follows that

$$\begin{aligned}\hat{W}_0(x|\omega)=&\frac{1}{2B^4(\omega)[1+\cos B(\omega)\cosh B(\omega)]}\\&\times(-2-2\cos B(\omega)\cosh B(\omega)\\&+\cos(B(\omega)x)+\cosh(B(\omega)x)+\cos(B(\omega)\\&\times[1-x])\cosh B(\omega)+\cos B(\omega)\cosh(B(\omega)\\&\times[1-x])-\sin(B(\omega)[1-x])\sinh B(\omega)\\&+\sin B(\omega)\sinh(B(\omega)[1-x])),\end{aligned}\tag{B4}$$

where $B(\omega)$ is defined in Eq. (15). Substituting Eq. (B4) into (B3) we obtain

$$\alpha_n(\omega)=\frac{2\sin C_n\tan C_n}{C_n(C_n^4-B^4(\omega))(\sin C_n+\sinh C_n)}.\tag{B5}$$

To calculate the magnitude of each driving force $\hat{F}_n(\omega)$, we use the property that the expectation value of the potential energy for each mode is $1/2k_BT$. Consequently, we refer to the general expression for the potential energy $U(t)$ of the beam,

$$U(t)=\frac{1}{2}\frac{EI}{L^3}\int_0^1\left(\frac{\partial^2 w(x,t)}{\partial x^2}\right)^2dx.\tag{B6}$$

From Eq. (B2), it is clear that $w(x,t)$ is given by

$$w(x,t)=\sum_{n=1}^{\infty}\beta_n(t)\phi_n(x),\tag{B7}$$

where $\beta_n(t)$ is the inverse Fourier transform of $\hat{F}_n(\omega)\alpha_n(\omega)$. Since $\phi_n(x)$ satisfy Eq. (B1), and the boundary conditions given in Eq. (4), it then follows that the potential energy of each mode $U_n(t)$ is given by

$$U_n(t)=\frac{1}{2}\frac{EI}{L^3}\beta_n^2(t)\int_0^1\left(\frac{d^2\phi_n(x)}{dx^2}\right)^2dx.\tag{B8}$$

From this expression and Eq. (24), the expectation value of the potential energy of each mode $\langle U_n(t)\rangle$ can be directly calculated and equated with $1/2k_BT$, from which we obtain

$$\tfrac{1}{2}k_BT=\tfrac{1}{6}kC_n^4\langle\beta_n^2(t)\rangle,\tag{B9}$$

where k is the spring constant of the beam and is given by

$$k=\frac{3EI}{L^3}.\tag{B10}$$

Since $\beta_n(t)$ is the inverse Fourier transform of $\hat{F}_n(\omega)\alpha_n(\omega)$, it is then follows that

$$\langle\beta_n^2(t)\rangle=\frac{1}{2\pi}\int_{-\infty}^{\infty}|\hat{F}_n(\omega')|_s^2|\alpha_n(\omega')|^2d\omega'.\tag{B11}$$

Substituting Eq. (B11) into (B9) and rearranging, we find

$$|\hat{F}_n(\omega)|_s^2=\frac{3\pi k_BT}{kC_n^4\int_0^{\infty}|\alpha_n(\omega')|^2d\omega'}.\tag{B12}$$

Finally, noting that all modes are uncorrelated, it follows from Eqs. (B12) and (B2) that the magnitude of $\hat{W}(x|\omega)$ is given by

$$|\hat{W}(x|\omega)|_s^2=\frac{3\pi k_BT}{k}\sum_{n=1}^{\infty}\frac{|\alpha_n(\omega)|^2}{C_n^4\int_0^{\infty}|\alpha_n(\omega')|^2d\omega'}\phi_n^2(x),\tag{B13a}$$

whereas the magnitude of the slope of $\hat{W}(x|\omega)$ is

$$\begin{aligned}\left|\frac{\partial\hat{W}(x|\omega)}{\partial x}\right|_s^2=&\frac{3\pi k_BT}{k}\sum_{n=1}^{\infty}\frac{|\alpha_n(\omega)|^2}{C_n^4\int_0^{\infty}|\alpha_n(\omega')|^2d\omega'}\\&\times\left(\frac{d\phi_n(x)}{dx}\right)^2.\end{aligned}\tag{B13b}$$

Equations (B13a) and (B13b) are the required results.

[1] W.-H. Chu, Tech. Rep. No. 2, DTMB, Contract NObs-86396(X), Southwest Research Institute, San Antonio, Texas (1963).
[2] U. S. Lindholm, D. D. Kana, W.-H. Chu, and H. N. Abramson, J. Ship Res. **9**, 11 (1965).
[3] D. G. Stephens and M. A. Scavullo, NASA TN D-1865 (April 1965).
[4] L. Landweber, J. Ship Res. **11**, 143 (1967).
[5] W. E. Newell, Science **161**, 1320 (1968).
[6] A. T. Jones, Exp. Mech. **10**, 84 (1970).
[7] L. Landweber, J. Ship Res. **15**, 97 (1971).
[8] G. Muthuveerappan, N. Ganesan, and M. A. Veluswami, J. Sound Vib. **61**, 467 (1978).
[9] D. G. Crighton, J. Sound Vib. **87**, 429 (1983).
[10] G. Muthuveerappan, N. Ganesan, and M. A. Veluswami, Comput. Struct. **21**, 479 (1985).
[11] Y. Fu and W. G. Price, J. Sound Vib. **118**, 495 (1987).
[12] R. E. Hetrick, Sens. Actuators **18**, 131 (1989).
[13] T. Tschan and N. de Rooij, Sens. Actuators A **32**, 375 (1992).
[14] H.-J. Butt, P. Siedle, K. Seifert, K. Fendler, T. Seeger, E. Bamberg, A. L. Weisenhorn, K. Goldie, and A. Engel, J. Microsc. **169**, 75 (1993).
[15] B. Abedian and M. Cundari, Proc. SPIE **1916**, 454 (1993).
[16] G. Y. Chen, R. J. Warmack, T. Thundat, and D. P. Allison, Rev. Sci. Instrum. **65**, 2532 (1994).
[17] J. E. Sader, I. Larson, P. Mulvaney, and L. R. White, Rev. Sci. Instrum. **66**, 3789 (1995).
[18] D. A. Walters, J. P. Cleveland, N. H. Thomson, P. K. Hansma, M. A. Wendman, G. Gurley, and V. Elings, Rev. Sci. Instrum. **67**, 3583 (1996).
[19] T. E. Schaffer, J. P. Cleveland, F. Ohnesorge, D. A. Walters, and P. K. Hansma, J. Appl. Phys. **80**, 3622 (1996).
[20] H. Muramatsu, N. Chiba, K. Homma, K. Nakajima, T. Ataka, S. Ohta, A. Kusumi, and M. Fujihira, Thin Solid Films **273**, 335 (1996).
[21] A. Roters and D. Johannsmann, J. Phys.: Condens. Matter **8**, 7561 (1996).
[22] M. K. Kwak, Trans. ASME, J. Appl. Mech. **63**, 110 (1996).
[23] T. E. Schaffer, M. Viani, D. A. Walters, B. Drake, E. K. Runge, J. P. Cleveland, M. A. Wendman, and P. K. Hansma, Proc. SPIE **3009**, 48 (1997).
[24] F.-J. Elmer and M. Dreier, J. Appl. Phys. **81**, 7709 (1997).
[25] M. Tortonese and M. Kirk, Proc. SPIE **3009**, 53 (1997).
[26] L. D. Landau and E. M. Lifshitz, *Theory of Elasticity* (Pergamon, Oxford, 1970).
[27] This is directly applicable to cantilever beams of small dimensions, such as those encountered in the atomic force microscope.
[28] T. R. Albrecht, S. Akamine, T. E. Carver, and C. F. Quate, J. Vac. Sci. Technol. A **8**, 3386 (1990).
[29] K. E. Petersen and C. R. Guarnieri, J. Appl. Phys. **50**, 6761 (1979).
[30] H.-J. Butt and M. Jaschke, Nanotechnology **6**, 1 (1995).
[31] M. V. Salapaka, H. S. Bergh, J. Lai, A. Majumdar, and E. McFarland, J. Appl. Phys. **81**, 2480 (1997).
[32] J. L. Hutter and J. Bechhoefer, Rev. Sci. Instrum. **64**, 1868 (1993).
[33] J. W. M. Chon, P. Mulvaney, and J. E. Sader (in preparation).

[34] This condition can be satisfied even for beams with salient edges, since in practice the radius of curvature of such edges is never zero.
[35] L. D. Landau and E. M. Lifshitz, *Fluid Mechanics* (Pergamon, Oxford, 1975).
[36] G. K. Batchelor, *Fluid Dynamics* (Cambridge University Press, Cambridge, UK, 1974).
[37] The convention adopted for the Reynolds number is in line with Ref. 36. We point out that the Reynolds number is often associated with the nonlinear convective inertial term of the Navier Stokes equation. This latter convention has not been adopted here.
[38] P. M. Morse and H. Feshbach, *Methods of Theoretical Physics* (McGraw-Hill, New York, 1953).
[39] L. Rosenhead, *Laminar Boundary Layers* (Clarendon, Oxford, 1963).
[40] For consistency with Eq. (6), the oscillations have a time dependence given by $\exp(-i\omega t)$, corresponding to a forward traveling wave.
[41] M. Abramowitz and I. A. Stegun, *Handbook of Mathematical Functions* (Dover, New York, 1972).
[42] R. P. Kanwal, Z. Angew. Math. Mech. **35**, 17 (1955).
[43] E. O. Tuck, J. Eng. Math. **3**, 29 (1969).